Dynamics of HCl Collisions with Hydroxyl- and Methyl-Terminated Self-Assembled Monolayers†

James R. Lohr, B. Scott Day, and John R. Morris*

Department of Chemistry, Virginia Tech, Blacksburg, Virginia 24061

Received: August 1, 2005; In Final Form: September 26, 2005

Molecular beam scattering techniques are used to explore the energy exchange and thermal accommodation efficiencies of HCl in collisions with long-chain OH- and CH_3-terminated self-assembled monolayers (SAMs) on gold. Upon colliding with the nonpolar methyl-terminated SAM, HCl ($E_i = 85$ kJ/mol) is found to transfer the majority, 83%, of its translational energy to the surface. The extensive energy loss for HCl helps to bring the molecules into thermal equilibrium with the monolayer. Specifically, 72% of the HCl approaches thermal equilibrium prior to desorption. For the molecules that do not thermally accommodate, but scatter after an impulsive collision with the surface, the final translational energy is observed to be directly proportional to the surface temperature as the thermal surface energy and gas translational energy exchange during the collision. For the OH-terminated SAM, the impulsively scattered HCl escapes from the surface with slightly more average energy. The rigid nature of the OH-terminated SAM is due to the extended intra-monolayer hydrogen-bonding network that restricts some of the low-energy modes of the surface. However, despite the rigid nature of this system, the extent of thermal accommodation for HCl on these two surfaces is remarkably similar. It appears that the potential energy well between the impinging HCl and the polar surface groups is sufficient enough to trap HCl molecules that would otherwise scatter impulsively from this rigid SAM.

1. Introduction

The transport of gases across hydrocarbon surfaces plays an important role in atmospheric chemistry. Studies have demonstrated that organic and surfactant-covered aerosols are abundant in many regions of the troposphere.[1−6] The surfaces of these particles are initially hydrophobic when formed, but oxidative reactions may make them more hydrophilic by incorporating carboxylic acid and other functional groups into the materials.[7−15] The dissolution of atmospheric $HCl_{(g)}$ into these and other particles, like water droplets and ice crystals, plays an important role in the overall chemistry of the atmosphere. Hydroxyl sites on the surfaces can help bind gas-phase HCl through hydrogen-bonding interactions, initiate a reaction by accepting an HCl proton, or serve as a surface-bound reagent for other reactions.[16] Each of these processes is mediated by an initial gas−surface collision, where the subsequent fate of the HCl molecule depends on the dynamics of the interaction. Our objective is to probe the nature of HCl surface collisions to help build a fundamental understanding of energy exchange, accommodation, and trapping when HCl collides with functionalized organic surfaces containing polar and nonpolar groups. These studies are facilitated by molecular beam scattering techniques to provide a well-characterized source of gas and self-assembled monolayers to present a well-characterized surface containing functional groups located precisely at the interface.

The transport of gas-phase molecules across an interface is regulated by the initial gas−surface collision where the energy exchange dynamics determine whether the molecule scatters impulsively or dissipates its energy to become trapped at the surface. Several recent experimental and theoretical studies have provided new insights into the mechanisms of gas−surface energy exchange and thermal accommodation for nonreactive collisions on organic surfaces. The computational studies of Hase et al. have contributed a great deal to our understanding of how the properties of organic surfaces influence the fate of interfacial collisions.[17−22] They have demonstrated that low-energy extended motions of alkane chains play the largest role in dissipating the energy of a gas−surface collision, whereas the high-energy C−H motions are not very active in the scattering dynamics.[23] The simulations have also provided new information about the nature of the low-energy scattering channel often described as trapping-desorption (TD). They find that for neon scattering from a methyl-terminated self-assembled monolayer (SAM), the apparent low-energy component to the energy distribution does not arise from an actual trapping-desorption intermediate. Rather, the low-energy scattered atoms leave the surface with a nonstatistical distribution of energies and recoil directions.[24] However, more polarizable gases such as Ar and Xe are found to scatter in two distinct pathways corresponding to direct inelastic and actual trapping-desorption channels.[25]

The molecular beam scattering experiments of Sibener et al. have also revealed significant insights into the dynamics of gas collisions on organic surfaces.[20,25,26] Their studies, often coupled with classical trajectory simulations, have helped to elucidate the specific vibrational modes that are important in Ar collisions with methyl-terminated SAMs. In addition, they have demonstrated that the interaction times of Ar with a self-assembled monolayer are very short. Impulsively scattered species are found to recoil from the surface after only 1 ps, and the time scales for normal and parallel momentum accommodation are also on the picosecond time scale.[20,25,26]

Recent theoretical studies of Ar collisions with CH_3-terminated SAMs by Troya and co-workers have furthered our understanding of the scattering dynamics for nonreactive gas−

† Part of the special issue "William Hase Festschrift".

* To whom correspondence should be addressed. E-mail: morris@vt.edu.

10.1021/jp0542625 CCC: $33.50
Published on Web 12/27/2005

surface collisions.[27] Their results have highlighted the importance of the potential energy surface in governing the outcome of the collision. Specifically, they find that differences in the gas−surface well-depth of only 1−2 kJ/mol can have a significant effect on the scattering dynamics, even for collision energies of 80 kJ/mol.[27] These results suggest that the dynamics for molecules such as HCl scattering from organic surfaces may depend a great deal on the polarity of the surface as dipole−dipole and hydrogen-bonding forces may contribute to the potential energy landscape.

The molecular beam studies of Pettersson et al. demonstrated that HCl efficiently transfers its incident energy to the surface of ice and HCl-doped ice.[28] They discovered three competing scattering channels for the surface interaction: direct inelastic scattering, trapping followed by prompt desorption, and long-time uptake. Comparisons of the HCl energy exchange and accommodation efficiencies to those for Ar scattering from ice revealed that the two gases followed very similar dynamics.[29,30]

Our previous studies for HCl scattering on well-ordered hydroxylated SAMs also show evidence for three distinct scattering channels.[31] We find that 85 kJ/mol HCl can scatter impulsively from the OH-terminated monolayer or dissipate its energy to thermally equilibrate on the surface. The accommodated molecules either desorb immediately back into the vapor phase or become trapped through the formation of HO••HCl hydrogen bonds. Comparisons with Ar scattering from ω-functionalized SAMs[32] suggest that the HCl-surface hydrogen-bonding and possibly dipole−dipole forces may play a major role in controlling the overall energy transfer and the overall accommodation efficiency on the surface.

The molecular beam scattering studies described below are aimed at providing further insight into the importance of gas−surface forces, such as hydrogen-bonding and dipole−dipole interactions, in controlling the fate of HCl in collisions with organic surfaces. The experiments focus on the dynamics of HCl impinging on CH_3- and OH-terminated self-assembled monolayers. These long-chain SAMs have nearly identical packing densities and structures but differ in their polarity at the gas−solid interface. Although previous studies have demonstrated that the OH-terminated monolayer is a more rigid partner for rare-gas collisions than the analogous CH_3-terminated SAM,[32,40] our results show that HCl thermally equilibrates more readily on the polar surface than the pure hydrocarbon surface. These results suggest that the gas−surface hydrogen-bonding and/or dipole−dipole interactions between HCl and OH groups are significant enough to overcome the rigid nature of the SAM.

2. Experimental Section

SAM Preparation. The SAMs used in this study were prepared by spontaneous chemisorption of hexadecanethiol ($HS(CH_2)_{16}CH_3$) and 16-mercapto-1-hexadecanol ($HS(CH_2)_{15}OH$) from 1 mM ethanolic solutions onto clean Au surfaces.[33] The chemicals used in this study were purchased from Aldrich and used without further purification. The substrates were prepared by Au evaporation onto Cr-coated glass slides (EMF Corp.). The gold-coated glass slides were cleaned in a piranha solution (70/30 (v/v) mixture of H_2SO_4/H_2O_2) prior to use. The clean gold slides were placed in the solutions for at least 12 h, rinsed with copious amounts of ethanol, dried under a stream of ultrahigh-purity nitrogen, and then immediately transferred to the main ultrahigh-vacuum chamber (base pressure $< 5 \times 10^{-10}$ Torr) via a load-lock system. In the main chamber, the samples are mounted on a precision manipulator that is in thermal contact with a liquid nitrogen reservoir and a sample heater that provides control over the surface temperature from 155 to 500 K. The sample temperature is measured by a K-type thermocouple spot-welded adjacent to the monolayer surface samples. Previous experiments from our group have shown that alkanethiol SAMs on gold-coated glass slides produce similar scattering results to the same studies performed for alkanethiols adsorbed onto atomically flat vapor-deposited gold on freshly cleaved mica.[32]

Molecular Beam Scattering. The experimental setup is similar to molecular beam scattering systems described previously.[32,34,35] High-energy HCl beams are created by expanding 2% HCl in H_2 at 700 Torr through a 0.05 mm diameter nozzle (General Valve). After passing through a 0.40 mm diameter conical skimmer located 6 mm from the nozzle, the beam enters a differential pumping stage where it collides with a mechanical chopper wheel. The slotted wheel, rotating at 185 Hz, produces approximately 80 μs pulses of gas that then pass through a 1.5 mm collimating aperture and into a final differential pumping stage. The final pumping stage is separated from the main ultrahigh-vacuum chamber by a 2.2 mm aperture through which the beam passes to produce a 1 cm^2 spot size on the surface sample located in the main chamber, 36 cm from the nozzle. The peak energy of the 2% HCl in H_2 mixture is $E_i = 85$ kJ/mol, as measured by recording the time-of-flight (TOF) distribution for a modulated beam directed at an in-line mass spectrometer.

The surface samples are aligned such that the normal is coplanar with the source and detector and at $\theta_i = 30°$ to the molecular beam. A fraction of the HCl that scatters from the surface is intercepted by a doubly differentially pumped mass spectrometer oriented at 60° to the incident beam such that $\theta_f = 30°$. The ionizer of the mass spectrometer views a 1 cm^2 spot size on the surface through two collimating apertures. The TOF distributions of the scattered HCl are determined by monitoring the mass spectrometer signal at $m/z = 36$ as a function of time. Each TOF scan is initiated when a slit of the chopper wheel passes a light-emitting diode (LED)−photodiode arrangement that sends a voltage pulse to trigger a multichannel scalar (Ortec). The multichannel scalar integrates signal from the spectrometer in 10 μs intervals.

The intensities and shapes of the TOF spectra were found to be highly stable and reproducible over the course of these studies. The stability in the experiments enables studies to be performed on surfaces at several different temperatures under identical conditions, facilitating direct comparisons of TOF spectra on relative scales. For Figures 2 and 3, we performed the measurements during the course of a 2 h period to minimize the effects of any slight changes in the beam intensity or mass spectrometer efficiency that may occur over much longer periods of time. In addition, the scattering studies shown in Figure 2, for which two different SAMs are directly compared, were conducted by mounting the two surface samples on the same sample holder and installing them into the ultrahigh-vacuum scattering chamber at the same time. We switched rapidly from one surface to the other by a simple translation of the sample manipulator.

3. Results and Discussion

HCl Scattering from CH_3-Terminated SAMs. Figure 1a shows TOF data for the 85 kJ/mol HCl beam scattering from the CH_3-terminated SAM. The data are a plot of the detector signal at $m/z = 36$ versus the flight time for molecules to traverse the distance between the surface and the ionizer of the mass spectrometer. The raw signal is proportional to number density $N(t)$ and is used to compute the probability $P(E_f)$ that an HCl

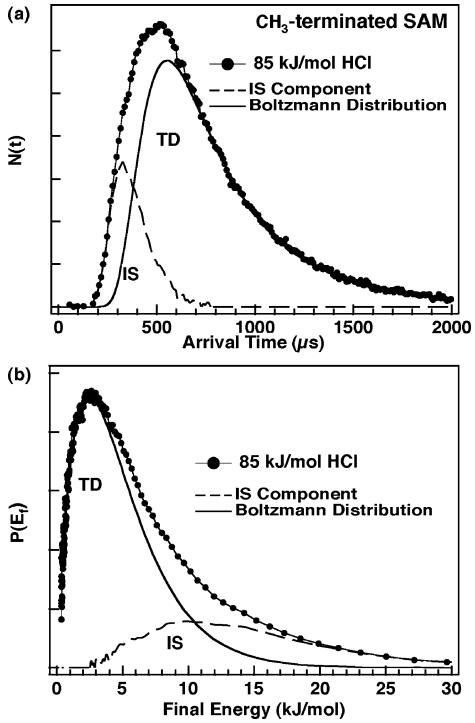

Figure 1. (a) TOF spectrum, $N(t)$, for 85 kJ/mol HCl scattering from a $HS(CH_2)_{15}CH_3$ SAM on Au at a surface temperature of 295 K. (b) The corresponding final translational energy distribution $P(E_f)$ was derived from the TOF data in a.

TABLE 1: Summary of Results for 85 kJ/mol HCl and 80 kJ/mol Ar Scattering from SAMs

gas→monolayer	TD fraction	IS energy transfer $(E_i - \langle E_{IS}\rangle)/E_i$
$HCl \rightarrow CH_3(CH_2)_{15}S-Au$	$0.72 \pm .01$	$0.83 \pm .01$
$HCl \rightarrow OH(CH_2)_{15}S-Au$	$0.74 \pm .01$	$0.78 \pm .01$
$Ar \rightarrow CH_3(CH_2)_{15}S-Au$	$0.61 \pm .01$ [32]	$0.83 \pm .01$ [32]
$Ar \rightarrow OH(CH_2)_{15}S-Au$	$0.43 \pm .01$ [32]	$0.77 \pm .01$ [32]

molecule leaves the surface with final energy E_f. The translational energy distributions are computed from the relations $E_f = (1/2)m_{HCl}(L/t)^2$ and $P(E_f) \sim t^2N(t)$, where t is the HCl flight time and L is the flight length. Figure 1b shows this translational energy distribution, $P(E_f)$. The distribution is separated into a direct-inelastic scattering (IS) component and a thermal accommodation component by assigning the latter component to the part that falls within a Boltzmann distribution: $P_{TD}(E_f) = E_f(RT_s)^{-2}\exp(-E_f/RT_s)$. The Boltzmann distributions in Figure 1a,b are represented by the solid curves. The excellent match of the Boltzmann curve to the low-energy portion of the scattering data strongly suggests that the molecules that contribute to the distribution at these energies are representative of a true TD channel, similar to that for Ar scattering from methyl-terminated SAMs.[25] The direct inelastic component to the energy distribution is assigned to the difference between $P(E_f)$ and $P_{TD}(E_f)$. The TD fraction, defined as the weighting coefficient, α, in the relation $P(E_f) = \alpha P_{TD}(E_f) + (1 - \alpha)P_{IS}(E_f)$,[36] is 0.72 ± 0.01 and the fractional energy transfer to the surface in the direct inelastic channel is $(E_i - \langle E_{IS}\rangle)/E_i = 0.83 \pm 0.01$. These results, along with scattering from the OH-terminated SAM, are summarized in Table 1.

The extensive energy exchange and thermal accommodation observed for HCl collisions with the CH_3-terminated SAM is the result of very efficient coupling of the translational energy of the impinging molecule to isolated and concerted motions of the methylene chains within the monolayer. The SAM

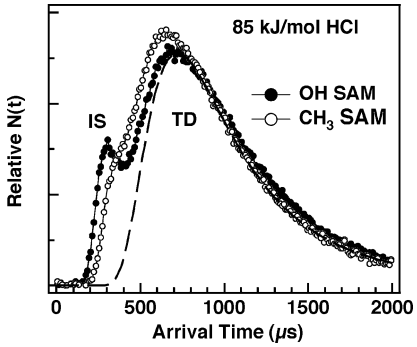

Figure 2. TOF distributions for 85 kJ/mol HCl scattering from CH_3- and OH-terminated SAMs at a surface temperature of 240 K. The dashed line represents a Boltzmann distribution at the surface temperature.

provides several degrees of freedom into which the translational energy of the impinging molecules can be partitioned. The bending motions of the chains, vibrational modes along the chains, and wags or rotations of the terminal groups can all be excited by the high-energy HCl.[20,21,23]

The significant energy transfer and thermal accommodation efficiency for HCl is very similar to the dynamics observed for Ar scattering from a CH_3-terminated SAM. For an 80 kJ/mol Ar beam impinging on a CH_3-terminated monolayer under the same experimental conditions as those used to record the data in Figure 1, we measured the TD fraction to be 0.61 and the fractional energy transfer to be 0.83.[32,37] The similar scattering dynamics for HCl and Ar impinging on the nonpolar hydrocarbon surface appear to be due to the kinematics rather than chemical forces, such that gases with similar size, mass, and incident energy follow similar scattering pathways.

Despite the similarities in the final energy distributions for HCl and Ar, HCl does exhibit a greater TD fraction than does Ar (0.72 as compared to 0.61). This difference may be due to a combination of factors related to the contrast in molecular versus atomic scattering. For example, HCl possesses internal degrees of freedom that can participate in the energy exchange event. Rotations and vibrations of the molecule are both energetically accessible for the high incident energy HCl. However, previous work has demonstrated that HCl vibrations are rarely excited in gas−surface collisions at energies around 80 kJ/mol,[38] and recent state-resolved scattering studies of CO_2 show that translational-to-vibrational energy transfer is very inefficient.[39] Therefore, the observed differences in Ar and HCl scattering are most likely due to differences in the gas−surface potential energy landscape and possibly rotations of the HCl.

Comparing Scattering from OH- and CH_3-Terminated SAMs. Previous results for Ar scattering show that OH-terminated SAMs and other associated polar surfaces are notably more rigid than analogous CH_3-terminated SAMs.[32,40] We find significantly lower TD fractions and higher energy IS distributions for Ar scattering from SAMs containing end groups that can form a hydrogen-bonding network. For example, the TD fraction for Ar scattering from a long-chain OH-terminated SAM is only 0.43 and $(E_i - \langle E_{IS}\rangle)/E_i = 0.77$.[32] In general, it appears that the hydrogen-bonding network anchors the end groups of an alkanethiol SAM to restrict some of the low-energy modes typically active in simple methyl-terminated monolayers.[32,41,42] However, the dynamics for HCl scattering from the hydrogen-bonding and non-hydrogen-bonding SAMs are markedly different than those observed for Ar.

Figure 2 shows a direct comparison of the TOF distributions recorded for HCl scattering from the OH- and CH_3-terminated

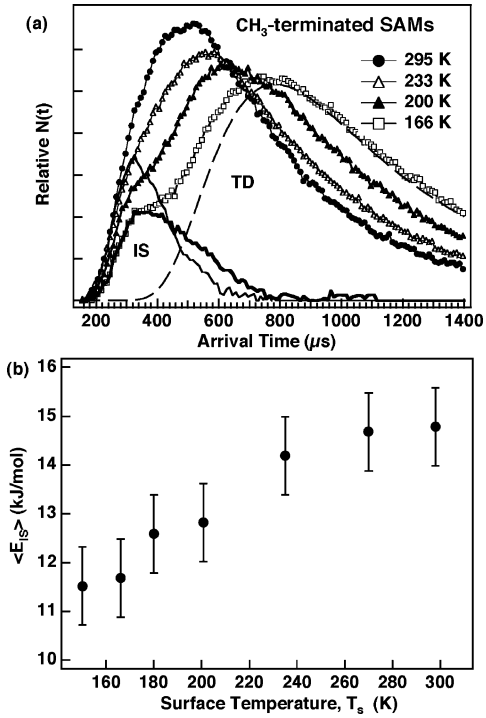

Figure 3. (a) Four TOF distributions (plotted on a relative scale) recorded at different surface temperatures. The IS components for T_s = 295 and 166 K are shown by the thin and thick lines, respectively. The dashed line is a Maxwell−Boltzmann distribution for T_s = 166 K. (b) The average final energy in the IS channel for HCl scattering from CH_3-terminated SAMs versus surface temperature.

monolayers. Although the average final energy in the IS channel is higher (as evidenced by earlier arrival times) for HCl recoiling from the OH-terminated SAM (in agreement with the trend observed for Ar), the overall TOF distributions are remarkably similar. These observations suggest that as HCl collides with the OH-terminated SAM, some of the molecules experience a repulsive wall similar to that for Ar and recoil immediately from the surface to retain a relatively large fraction of their incident energy. However, most of the HCl molecules appear to transfer enough energy to the OH surface during the initial collision to become trapped in the gas−surface potential energy well. The trapping efficiency is different for Ar scattering because the Ar−OH well is much less attractive,[20,25,27] by a factor of about 20, than the HCl−OH SAM potential.[31]

Previous experiments in our group have used pulsed molecular-beam residence-time measurements of HCl on the OH-terminated SAM to determine the adsorption energy to be 24 kJ/mol.[31] Therefore, any of the molecules that transfer (E_i − 24 kJ/mol) = 61 kJ/mol of energy to the SAM during the collision may become trapped on the surface and contribute to the TD channel. In addition to the OH···HCl hydrogen bonds that help trap molecules on the surface, HCl can also interact with the polar surface through dipole−dipole forces. Although our experiments cannot distinguish between these two contributions to the dynamics, they both likely play a significant role in contributing to the attractive potential well that appears to be significant enough to overcome the rigid nature of this associated SAM. Molecular dynamics simulations are currently underway to explore these issues in more detail.

Surface Temperature Dependence. We have further explored the gas−surface energy exchange by recording TOF spectra at several different surface temperatures. Figure 3 shows the TOF distributions for HCl scattering from the CH_3-terminated SAM surface at 295, 233, 200, and 166 K. We find that, throughout this entire temperature range, the TD distribution can be modeled well by a Boltzmann distribution at the temperature of the surface. This result is fundamentally different from the dynamics for HCl scattering from an OH-terminated SAM. Figure 2 of ref 31 shows that as the surface temperature of an OH-terminated SAM is reduced, the TD component of the distribution broadens to the extent that it cannot be described by a single Boltzmann distribution. The time broadening of the HCl TD channel on the OH SAM is due to the extensive residence time of the molecules on the surface at T_s < 200 K. In contrast, the residence time for HCl on the methyl surface is so small that it is not reflected in the final TOF distributions. This indicates that the residence time is <1 μs and probably much shorter, as expected for thermal HCl on the nonpolar surface. In fact, calculations indicate that the minimum well-depth for HCl interacting with methane is only about 3.5 kJ/mol,[43] which, according to transition-state theory, would lead to a characteristic surface residence time of only about 1 ps, even at T_s = 150 K.

Despite the effect of surface temperature on the residence time for HCl desorbing from the OH-terminated SAM, the TD fractions and final energy distributions for the direct impulsive scattering are nearly independent of surface temperature. In contrast, the intensity of the TD channel increases and the final energy of the HCl in the IS channel decreases as the surface temperature is reduced for the CH_3-terminated SAM. The surface appears to become more effective at dissipating the impinging HCl energy at lower temperatures. This effect is evidenced by Figure 3a, which shows that the IS component for scattering from the CH_3-terminated SAM shifts to longer arrival times, or lower final energies, as the temperature of the surface is reduced. This trend is further highlighted in Figure 3b, which shows the average final energy of molecules in the IS channel versus the temperature of the surface. The increase in the average energy of the IS channel with increasing surface temperature is due to the increasing thermal motions of the surface molecules that impart more energy to the gas during the impulsive collision.[25,44,45]

In contrast to the pure hydrocarbon SAM, the IS distribution for 85 kJ/mol HCl collisions with the hydroxylated surface appears to be remarkably insensitive to surface temperature over the range of 350 to 160 K. Figure 2 of ref 31 shows that the peak arrival time of the IS distribution for 85 kJ/mol HCl scattering from the OH-terminated SAM is constant over the entire range of temperatures studied. We find similar behavior for Ar scattering from the methyl- and hydroxyl-terminated SAMs. It appears that the hydrogen-bonding network restricts the types of thermal motions that couple to the translational energy of the impulsively scattered molecules. This interpretation is consistent with recent He atom scattering experiments, which showed direct evidence that the average thermal displacement increases more quickly with temperature for a methyl-terminated monolayer relative to an associated hydrogen-bonding system.[46] The picture that emerges from these scattering studies is that thermal motions of the surface molecules have a small effect on the dynamics and that this influence is readily dampened out by the presence of a rigid hydrogen-bonding network that restricts some of the thermal vibrations.

4. Summary

Molecular beam studies of the energy exchange and thermalization probabilities for HCl scattering from CH_3- and OH-terminated self-assembled monolayers have been used to learn about the role of gas−surface attractive forces in determining

the fate of these interfacial collisions. As high-energy HCl (E_i = 85 kJ/mol) collides with the CH_3-terminated SAM, it transfers the majority of its incident energy to the surface and over 70% of the molecules appear to completely thermally equilibrate with the monolayer. The large-energy exchange efficiency is due to the many low-energy vibrational and wagging motions that are excited during the collision. In contrast, impulsively scattered HCl resulting from collisions with the OH-terminated monolayer escapes from the surface with slightly more average energy. The rigid nature of the OH-terminated SAM is due to the extended intramonolayer hydrogen-bonding network that restricts some of the low-energy modes of the surface. However, the rigid nature of this system has only a minor influence on the overall thermalization probability relative to the CH_3-terminated SAM. It appears that the gas−surface hydrogen-bonding and dipole−dipole forces are strong enough to overcome the rigid nature of this SAM to trap a major fraction of the molecules that would otherwise scatter impulsively from the surface.

Acknowledgment. Funding for this work was provided by the National Science Foundation (CAREER Award No. CHE-94269). We would also like to thank Professor Diego Troya for very helpful discussions. The authors would like to especially thank Professor Bill Hase for his leadership in this field, which provided much of the motivation for our work. His insights continue to have a broad impact on our understanding of gas-surface scattering dynamics.

References and Notes

(1) Murphy, D. M.; Thomson, D. S.; Mahoney, T. M. J. *Science* **1998**, *282*, 1664.
(2) Novakov, T.; Penner, J. E. *Nature* **1993**, *365*, 823.
(3) Novakov, T.; Corrigan, C. E.; Penner, J. E.; Chuang, C. C.; Rosario, O.; Bracero, O. L. M. *J. Geophys. Res., [Atmos.]* **1997**, *102*, 21307.
(4) Cruz, C. N.; Pandis, S. N. *J. Geophys. Res., [Atmos.]* **1998**, *103*, 13111.
(5) Larson, S. M.; Cass, G. R.; Gray, H. A. *Aerosol Sci. Technol.* **1989**, *10*, 118.
(6) Gray, H. A.; Cass, G. R.; Huntzicker, J. J.; Heyerdahl, E. K.; Rau, J. A. *Environ. Sci. Technol.* **1986**, *20*, 580.
(7) Claeys, M.; Wang, W.; Ion, A. C.; Kourtchev, I.; Gelencser, A.; Maenhaut, W. *Atmos. Environ.* **2004**, *38*, 4093.
(8) Jang, M.; Czoschke, N. M.; Northcross, A. L. *Chemphyschem* **2004**, *5*, 1647.
(9) Iinuma, Y.; Boge, O.; Gnauk, T.; Herrmann, H. *Atmos. Environ.* **2004**, *38*, 761.
(10) Blando, J. D.; Porcja, R. J.; Li, T. H.; Bowman, D.; Lioy, P. J.; Turpin, B. J. *Environ. Sci. Technol.* **1998**, *32*, 604.
(11) Saxena, P.; Hildemann, L. M. *Environ. Sci. Technol.* **1997**, *31*, 3318.
(12) Hoffmann, T.; Odum, J. R.; Bowman, F.; Collins, D.; Klockow, D.; Flagan, R. C.; Seinfeld, J. H. *J. Atmos. Chem.* **1997**, *26*, 189.
(13) Odum, J. R.; Hoffmann, T.; Bowman, F.; Collins, D.; Flagan, R. C.; Seinfeld, J. H. *Environ. Sci. Technol.* **1996**, *30*, 2580.
(14) Saxena, P.; Hildemann, L. M. *J. Atmos. Chem.* **1996**, *24*, 57.
(15) Saxena, P.; Hildemann, L. M.; McMurry, P. H.; Seinfeld, J. H. *J. Geophys. Res., [Atmos.]* **1995**, *100*, 18755.
(16) Robinson, G. N.; Worsnop, D. R.; Jayne, J. T.; Kolb, C. E.; Swartz, E.; Davidovits, P. *J. Geophys. Res., [Atmos.]* **1998**, *103*, 25371.
(17) Yan, T. Y.; Hase, W. L.; Barker, J. R. *Chem. Phys. Lett.* **2000**, *329*, 84.
(18) Yan, T. Y.; Hase, W. L. *Phys. Chem. Chem. Phys.* **2000**, *2*, 901.
(19) Yan, T. Y.; Hase, W. L. *J. Phys. Chem. B* **2002**, *106*, 8029.
(20) Yan, T. Y.; Isa, N.; Gibson, K. D.; Sibener, S. J.; Hase, W. L. *J. Phys. Chem. A* **2003**, *107*, 10600.
(21) Yan, T. Y.; Hase, W. L.; Tully, J. C. *J. Chem. Phys.* **2004**, *120*, 1031.
(22) Bosio, S. B. M.; Hase, W. L. *J. Chem. Phys.* **1997**, *107*, 9677.
(23) Yan, T.; Hase, W. L. *J. Phys. Chem. B* **2002**, *106*, 8029.
(24) Yan, T.; Hase, W. L. *Phys. Chem. Chem. Phys.* **2000**, *2*, 901.
(25) Gibson, K. D.; Isa, N.; Sibener, S. J. *J. Chem. Phys.* **2003**, *119*, 13083.
(26) Isa, N.; Gibson, K. D.; Yan, T.; Hase, W.; Sibener, S. J. *J. Chem. Phys.* **2004**, *120*, 2417.
(27) Day, B. S.; Morris, J. R.; Troya, D. *J. Chem. Phys.* **2005**, *122*, 214712.
(28) Andersson, P. U.; Nagard, M. B.; Pettersson, J. B. C. *J. Phys. Chem. B* **2000**, *104*, 1596.
(29) Andersson, P. U.; Nagard, M. B.; Bolton, K.; Svanberg, M.; Pettersson, J. B. C. *J. Phys. Chem. A* **2000**, *104*, 2681.
(30) Bolton, K.; Svanberg, M.; Pettersson, J. B. C. *J. Chem. Phys.* **1999**, *110*, 5380.
(31) Lohr, J. R.; Day, B. S.; Morris, J. R. *J. Phys. Chem. B* **2005**, *109*, 15469.
(32) Day, B. S.; Shuler, S. F.; Ducre, A.; Morris, J. R. *J. Chem. Phys.* **2003**, *119*, 8084.
(33) Nuzzo, R. G.; Dubois, L. H.; Allara, D. L. *J. Am. Chem. Soc.* **1990**, *112*, 558.
(34) Ceyer, S. T.; Gladstone, D. J.; McGonigal, M.; Schulberg, M. T. *Molecular Beams: Probes of the Dynamics of Reactions on Surfaces*, 2nd ed.; Wiley: New York, 1988.
(35) Miller, D. R. *Atomic and Molecular Beam Methods*; Oxford University Press: New York, 1988; Vol. 1.
(36) Saecker, M. E.; Nathanson, G. M. *J. Chem. Phys.* **1993**, *99*, 7056.
(37) Day, B. S.; Morris, J. R. *J. Phys. Chem. B* **2003**, *107*, 7120.
(38) Chorny, I.; Benjamin, I.; Nathanson, G. M. *J. Phys. Chem. B* **2004**, *108*, 995.
(39) Perkins, B. G.; Haber, T.; Nesbitt, D. J. *J. Phys. Chem. B* **2005**, *109*, 16396.
(40) Shuler, S. F.; Davis, G. M.; Morris, J. R. *J. Chem. Phys.* **2002**, *116*, 9147.
(41) Ferguson, M. K.; Lohr, J. R.; Day, B. S.; Morris, J. R. *Phys. Rev. Lett.* **2004**, *92*, 073201.
(42) Day, B. S.; Davis, G. M.; Morris, J. R. *Anal. Chim. Acta* **2003**, *496*, 249.
(43) Troya, D. Private communication.
(44) Hurst, J. E.; Becker, J. P.; Cowin, K. C.; Jands, L. W.; Auerbach, D. J. *Phys. Rev. Lett.* **1979**, *43*, 1175.
(45) Harris, J. *Dynamics of Gas−Surface Interactions*; Royal Society of Chemistry: Cambridge, U.K., 1991.
(46) Bracco, G.; Acker, J.; Ward, M. D.; Scoles, G. *Langmuir* **2002**, *18*, 5551.